APPLICATION OF BEAM THEORY FOR THE CONSTRUCTION OF TWICE DIFFERENTIABLE CLOSED CONTOURS BASED ON DISCRETE NOISY POINTS

I. ORYNYAK, D. KOLTSOV, O. CHERTOV, R. MAZURYK

Abstract. The smoothing of measured noisy positions of discrete points has considerable significance in various industries and computer graphic applications. The idea of work consists of the employment of the technique of beam with spring supports. The local coordinates systems are established for beam straight line segments, where the initial angles between them are accounted for in the conjugation equations, which provide the angular continuity. The notions of imaginary points are introduced, the purpose of which is to approach the real length of the smoothed contour to the length of the straight chord. Several examples of closed denoised curve reconstruction from an unstructured and highly noisy 2D point cloud are presented.

Keywords: spline, elastic beam, spring support, closed contour, imaginary point, noisy data.

INTRODUCTION

Two cases are discerned at geometrical computer modeling of plane curves or closed contours – their design or restoration from the set of measured points. In each case the provision of the curves smoothness is a necessary requirement of their construction.

During geometrical design the important prerequisite is an aesthetical appeal and C^2 continuity of a curve. The most popular are the methods which are based on the Bezier curves, rational Bezier curves, B-splines and rational B-splines, or so-called NURBS curves [1]. For their construction it is needed to define the enumerated system of so-called control points. These curves pass exactly through the first and last points, while all other points are only attracting the curve to themselves. To increase or decrease the "weight" of attraction of the given control point the rational splines are applied.

The problem of restoration of closed curves from the noise points has a big significance in a computational geometry. It is applied in image analysis, in reverse engineering, for restoration of the trajectories and forces acting on the moving material points, etc. [2]. As an example, mention the extraction of silhouettes from sensed depth images.

Very often the restoration of the geometry is performed by fitting the points for the prescribed analytical figure (circle, ellipse, helix) with unknown characteristics, orientation and center of coordinates. In this case the functional of error (sum of deviations) is specified, which usually is iteratively solved by least square method [3]. When the number of points is too big it is necessary to perform the

preliminary smoothing. Then the weighting Gaussian probability function is usually applied, which makes the closer positions of the considered points [4]. Yet its application might lead to unpredictable loss of the useful information (over smoothing). Furthermore, the drawback of similar techniques is that the real noise of input points (mean deviation) is not taken into account, even if it is known in advance [4].

Historically the first splines which exactly pass through the given measured points were solutions based on the Strength of Materials beam technique [5] and actually used the known equation of three moments [6]. To decrease the deviation of the curves from the given points it was suggested to use the solutions for initially pre-tensed beams [7]. Later on, the theory of beam splines was supplemented by possibility to use the elastic springs (supports) placed in the points of measurements. The increase in compliance of these springs lead to larger smoothing of the resulting curve [8].

The most drawback of all beam based smoothing techniques is that the curve is presented in unique global coordinate system, i.e., the solution of kind $y = f(x)$ is searching for. Sush presentation can be effective for drawing the statistical splines, where the independent variable x is determined exactly, while the functions y can be presented in any scale. For geometrical splines both coordinated has the similar meaning and both are determined with errors. Usual approach is a parametrical presentation of both coordinates and execution the independent smoothing with respect to each coordinate.

Significant contribution to application of the theory of beams to the geometrical smoothing are works of present authors [9, 10], where the initial straight segments between the neighboring points predetermine the local coordinate and vector basis which are adjacent to each other at a certain angle. Namely, the goal of the beam deformation was the smoothing of these angles [9, 10]. Note, that idea of application of initial straight segments and their vectorial basis is the main one in so-called corotational approaches in geometrical nonlinear analysis of the spatial beams, when the position of the deformed geometry is essentially deviate from the initial one [11].

The peculiarity and main idea of given work consists in that beam spring splines are calculated iteratively with accounting for the big deviation and change of local basis vector system (tangent and normal) [12]. Besides the notion of fictitious points is introduced here which are not related with the real (measured) points. These points are placed on calculated contour between the real points for decreasing the angle between the neighboring segments.

GOVERNING EQUATIONS

Consider the simplest model of the bending deformation of beam, so called Euler-Bernoulli beam [6], its equations and parameters. Beam is described by the generalized vector of state $\vec{Y}(s)$, which characterized by set of four parameters at each local point of length coordinate s, i.e., $\vec{Y}(s) = column \{W(s); \theta(s); M(s); Q(s)\}$. Here, instead of some function and its derivatives, as usually accepted in mathematics, the following conventional parameters of the theory of beam are used. So,

we operate by notions of: $W(s)$ is the deviation or displacement, the positive value of which is directed toward the normal; $\theta(s)$ is the angle of rotation, the positive direction coincides with rotation from the tangent vector to normal one, i.e., is in clockwise direction; $M(s)$ is the bending moment; $Q(s)$ is transverse force. Their positive directions are chosen in such manner that in all differential equations the sign «+» is used. Thus, the following dependences between the beam parameters are used:

$$\frac{dW(s)}{ds} = \theta(s); \quad \frac{d\theta(s)}{ds} = \frac{M(s)}{EI}; \quad \frac{dM(s)}{ds} = Q(s); \quad \frac{dQ(s)}{ds} = q_m,$$

where q_m is given outer distributed force, EI is so called rigidity of the beam section. The solution of the system of governing equations is presented in form suitable for application of transfer matrix method, and is the following:

$$(\vec{Y}(s)) = \begin{bmatrix} 1 & s & \dfrac{s^2}{2EI} & \dfrac{s^3}{6EI} \\ 0 & 1 & \dfrac{s}{EI} & \dfrac{s^2}{2EI} \\ 0 & 0 & 1 & s \\ 0 & 0 & 0 & 1 \end{bmatrix} (\vec{Y}_0) + q_m \begin{pmatrix} \dfrac{s^4}{24EI} \\ \dfrac{s^3}{6EI} \\ \dfrac{s^2}{2} \\ s \end{pmatrix}, \tag{1}$$

where $\vec{Y}_0 = \vec{Y}(s=0)$ is the vector of state at initial point of the segment. Note that here we take that $EI \equiv 1$, and $q_m = 0$.

The set of measured positions of enumerated points $B_i(X_{bi}, Y_{bi})$ is a required input information, thus each point has number i, it is characterized by two coordinates position which are measured with some error characterized by some prescribed statistical deviation σ.

At each iteration number, j, the geometry of analyzed curve is presented as a set of points $A_i^j(X_i^j, Y_i^j)$, where each point A_i^j is related with initial point B_i with the same index i. Note, that before first iteration the positions of points $A_i^{j=0}$ coincide with those of measured points B_i. Usually, we will omit the upper index j in designation of points A_i. Consequent points A_i are connected by straight segments. These segments form certain angles between themselves, $\psi_{i-1,i}$, the positive directions of which is counted clockwise (Fig. 1). Thus, the beginning and end of each segment i, at each iteration, j, have some positions, which coincide with positions of points A_i (Fig. 1). The vectorial length of each segment is denoted as $\vec{L}_i$:

$$\vec{L}_i = \vec{A}_{i+1} - \vec{A}_i = (X_{i+1} - X_i)\vec{i} + (Y_{i+1} - Y_i)\vec{j}.$$

Each of these segments is related with local tangent vector $\vec{t}_i$ and normal vector $\vec{n}_i$, which is rotated clockwise with respect to former one. Thus, if the tangent vector $\vec{t}_i$ is given by:

$$\vec{t}_i(s) = \frac{\vec{L}_i}{\left|\vec{L}_i\right|} = a_i\vec{i} + b_i\vec{j} = \text{const}.$$

Then normal vector $\overrightarrow{n_i}$ is found from the expression:

$$\vec{n}_i(s) = c_i\vec{i} + d_i\vec{j} = b_i\vec{i} - a_i\vec{j} = \text{const}.$$
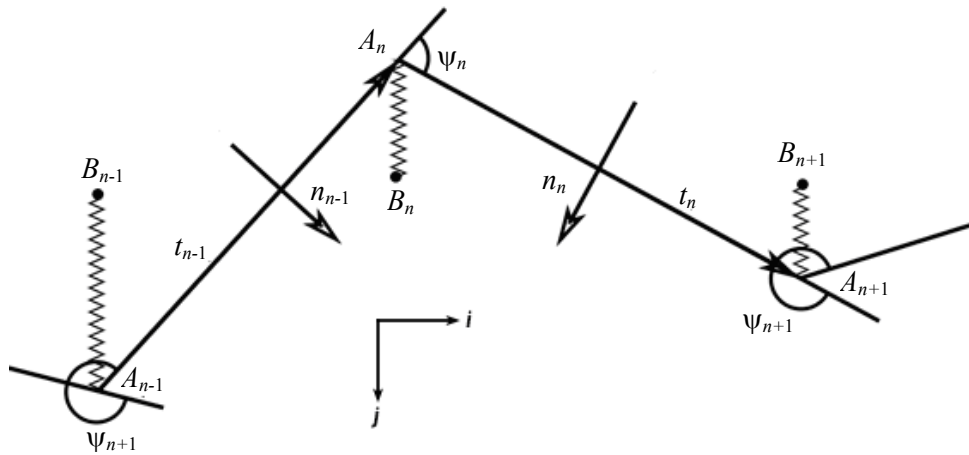

Fig. 1. The model of discrete beam segments on elastic springs (supports)

The important constituent of the modelling is accounting for the angle between two segments, name it as a misalignment angle. It must be smoothed at the next iteration. This angle is denoted as $\psi_{i-1,i}$, and its direction is clockwise, Fig 1, and calculated by the formulas of the vector and scalar products of the unit vectors:

$$\sin(\psi_{i,i-1}) = \vec{t}_i * \vec{t}_{i-1}; \qquad \cos(\psi_{i,i-1}) = \vec{t}_i\,\vec{t}_{i-1}.$$

We use both definitions of angle to get the correct values of it in each quadrant of the coordinate system. Note, that if both signs are positive, then angle lies in first quadrant, if both are negative – in third quadrant, and so on.

Formulate the main parameters, unknowns and equations which will be used in calculation.

Introduce the following designations for main parameters (unknowns at each iteration). At each segment, i, introduce the vector of state in initial point, thus $\vec{Y}_{i,0}(s = 0)$, and vector of state at the last point of segment, thus $\vec{Y}_{i,e}(s = s_i)$. Evidently, these two vectors of state are related by Connection equations (1), at $s = s_i = \left|\vec{L}_i\right|$.

The peculiarity of given approach consists in consideration of initial noisy points as the fixed positions of elastic supports, where the additional force of interaction is proportional to the deviation of the position of the contour point $\vec{A}_i$ from the support point B_i. This deviation is determined before the next iteration and designated as Π_i. Other peculiarity consists in accounting for the angle of

misalignment [10]. So, additionally to the Connection equations, write the Conjugation equations, which relate the vectors of state at the end of previous segment with that at the beginning of the next one:

$$W_{i+1,0} = W_{i,1};$$ (2)

$$\theta_{i+1,0} = \theta_{i,1} - \psi_{i,i+1};$$ (3)

$$M_{i+1,0} = M_{i,1};$$ (4)

$$Q_{i+1,0} = Q_{i,1} - C_i(W_{i,1} - \Pi_i),$$ (5)

where C_i is the rigidity of support (characteristic of spring), and Π_i is some conditional distance, the value of which before the first iteration is taken as $\Pi_i = 0$.

Equation (5) can lead to some computational errors when C_i is a very big. As alternative presentation of (5) we use relation

$$(W_{i,1} - \Pi_i) = D_i(Q_{i+1,0} - Q_{i,1}),$$ (6)

where the notion of the support's compliance D_i is introduced, which is inverse to the rigidity $D_i = C_i^{-1}$.

Comment these equations. First one (2) is intended for that displacements (positions) at the border between two segments should be equal — C^0 continuity. Second one (3) is intended for that angle of tangent to the next segment should be on value of $\psi_{i,i+1}$ lesser than the angle of tangent at the end of the previous one – actually this gives the angle continuity requirement of the deformed contour — C^1 continuity. Third condition (4) is a condition of continuity of second derivatives. The values of calculated $W_{i,1}$ and Π_i, the latter is being determined before each iteration by the special procedure, have the signs. The positive sign means that value is directed toward direction of vector $\vec{n}_i$. Note that at intermediate values of D_i and C_i the equations (5) and (6) are equivalent. If $C_i \gg 1$, then equation (6) should be used, which in limit case of $C_i \to \infty$, or $D_i \to 0$, actually leads to equation: $W_{i,1} = \Pi_i$. Similarly, there are no restrictions in applying of (6), when $C_i \to 0$, or $D_i \to \infty$, then equation (5) will be reduced to $Q_{i+1,0} = Q_{i,1}$.

Thus, if the whole number of measured points is equal to N, then we introduce N segments (the last one for closed contours connect the point $i = N$ with point $i = 1$). This means that at whole we have $2*4*N = 8N$ unknowns (two sets of four ones at the beginning and at the end of each segment). For determination of them there are N sets of Connection equations (1), thus $4N$ ones at the whole, and similarly $4N$ Conjugation equations (2) – (5).

MAIN IDEA OF ALGORITHM

Describe the procedure of consequent rebuilding of the smoothed contour at each iteration. The main result of calculation is deviation of points A_i from the previous positions, and they are designated as $\vec{W}_i$. According to Conjugation requirement (2):

$$\left|\vec{W}_i\right| = \left|\vec{W}_{i+1,0}\right| = \left|\vec{W}_{i,1}\right|.$$

Yet, evidently the displacements of beam, $W(s)$ are directed toward the normal to each straight segment, which are different for two adjacent segments. Thus, the vectorial displacements $\vec{W}_{i+1,0}$ and $\vec{W}_{i,1}$ are different:

$$\vec{W}_{i+1,0} = \left|\vec{W}_{i+1,0}\right|\vec{n}_{i+1} \neq \vec{W}_{i,1} = \left|\vec{W}_{i,1}\right|\vec{n}_i.$$

To provide the C^0 continuity of deformed contour we make the following original enhancement: namely, introduce the notion of continuous normal vectors to the calculated deformed geometry. They are derived by rotation of initial normal vectors on the calculated angle of deformation $\theta_i(s)$. We name them as deformed normal, denote them as $\overrightarrow{n\theta}_{i+1}$ and calculate by the following formula:

$$\overrightarrow{n\theta}_i(s) = \vec{n}_i \cos\theta(s) - \vec{t}_i \sin\theta(s) = c\theta_i(s)\vec{i} + d\theta_i(s)\vec{j}, \qquad (7)$$

where

$$\begin{pmatrix} c\theta_i(s) \\ d\theta_i(s) \end{pmatrix} = \begin{pmatrix} \cos(-\pi/2 - \theta(s)) & -\sin(-\pi/2 - \theta(s)) \\ \sin(-\pi/2 - \theta(s)) & \cos(-\pi/2 - \theta(s)) \end{pmatrix} \begin{pmatrix} a_i \\ b_i \end{pmatrix}.$$

Evidently, that due to condition (3) the deformed normal are continuous along the whole contour including the borders between adjacent elements, i.e. $\overrightarrow{n\theta}_{i+1}(s=0) = \overrightarrow{n\theta}_i(s=s_i)$. Then treating the calculated vectorial displacements as $\vec{W}_i(s) = W(s) \cdot \overrightarrow{n\theta}_i(s)$, we get that positions of two adjacent border points $\vec{A}_i^j$ will be continuous.

Accounting for continuity of displacements $W(s)$ and angle of deformation $\theta(s)$ calculate the position of each inner point of segment $\vec{R}_i^j(s)$, which is presented as the sum of initial position and calculated deformed position:

$$\vec{R}_i^j(s) = \vec{A}_i^{j-1} + \vec{t}_i \cdot s + W(s) \cdot \overrightarrow{n\theta}_i(s). \qquad (8)$$

Thus, formula (8) is a main formula to determine the positions of all points after each iteration. It may happen, that derived figure satisfy the requirements to the smoothed contour and we can stop the calculations immediately. But if the derived contour does not satisfy to the requirements, we have two options. First is a trivial one. We can start again the procedure from the first iteration, where $A_i^{j=0} = B_i$, but different value of rigidity C_i can be chosen: the smaller it is, the

smoother contour will be. This option is applicable when the deviation of measured points is small as compared with distance between them.

More complicated is the second option which requires the creation of additional refining procedures, and which is the main objective of our analysis. Consider that first iteration is already performed at initial (big) values of C_i, take them to be of the same value and designate as C_S. This results in derivation of new positions of points A_i. Connect these points, form new segments and derive new angles of misalignments. Take other (smaller) values of C_s and perform the next iteration.

Important to evaluate whether the given value of C_s is big or small. Evidently the value of C_s can be considered as a small one, when the calculated displacements W are small as compared with segment length. Theory of beams [6] states, that following property characterizes the dimensionless rigidity of spring, $\overline{C}_s = \dfrac{C_s \cdot L^3}{6EI}$. The spring is rigid if $\overline{C}_s > 1$, and is flexible if $\overline{C}_s < 1$. Thus, we initially chose some approximate mean value of length of all segments, L, and then we chose some initial big value of the rigidity, for example, $\overline{C}_s = 400$. Then real C_s is calculated as

$$C_s = \frac{6}{L^3}\overline{C}_s ,$$

because $EI = 1$.

To complete the preparation for the next iteration it is necessary to find the preliminary force of the spring tension, which is characterized by some conditional distance Π_i. If consider Π_i as the absolute distance between points $\vec{B}_i$ and $\vec{A}_i$, then some collisions could occur. It may happen that some point $\vec{B}_i$ lays on (or is very close to) the new contour, but is situated very far from related calculated point $\vec{A}_i$. In such treatment: a) the value of Π_i could be big, thus the large preliminary force will arise, although point $\vec{A}_i$ is very close to contour; b) it is not possible to define the sign of Π_i ("+" or "-"), which would lead to unpredictable results at the next iteration.

Then, value of Π_i is defined as the shortest distance from point $\vec{B}_i$ for both segments $\overrightarrow{A_{i-1}A_i}$ and $\overrightarrow{A_i A_{i+1}}$ with accounting for their signs. These two distances are designated as Π_{1i} and Π_{2i}, and are determined as: $\overrightarrow{A_i B_i} \cdot \vec{n}_{i-1} = \Pi_{1i}$; and $\overrightarrow{A_i B_i} \cdot \vec{n}_i = \Pi_{2i}$. The smallest by module of them is chosen as Π_i with accounting of its sign, so Π_i is taken with sign «+», if point B_i is situated at the right side from the respected segment and «-» otherwise.

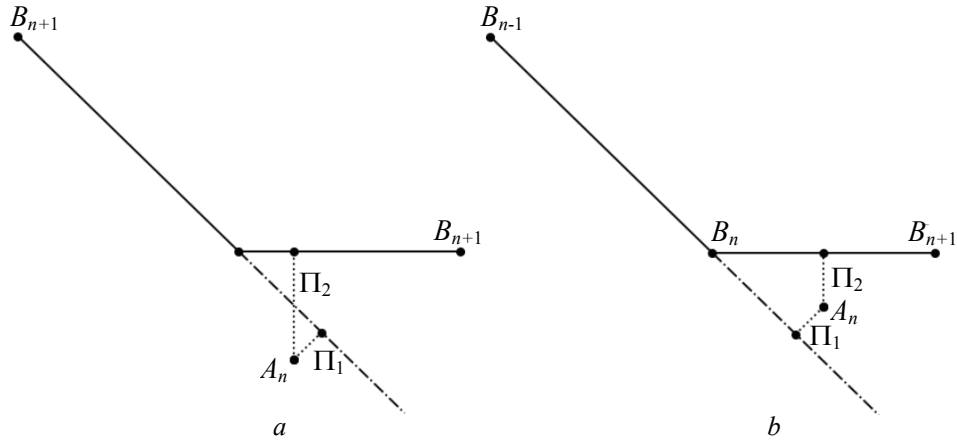Some cases of choosing the value of Π_i are shown on Fig. 2.

Fig. 2. Some cases of finding the distances from control point A to two straight segments: a — one distance is positive and other is negative; b — both distances are positive

REFINEMENT OF LENGTH AND CURVATURE AND IMAGINARY POINTS

Before j-th iteration we operate only by the positions of border points A_i^{j-1}. The main result of calculation at j-th iteration is position of each point s, where $0 \le s \le s_i$, of the segment (8). Analyze the change of length of infinitely small straight element Δs of the segment after deformation. Rewrite the expression (8) with accounting for (7):

$$\vec{R}_i^j(s) = \vec{A}_i^{j-1} + \vec{t}_i^{j-1} X(s) + \vec{n}_i^{j-1} Y(s), \qquad (9)$$

where

$$X(s) = (s - W(s)\sin\theta(s)), \ Y(s) = W(s)\cos\theta(s).$$

These formulas give the position of each point s. Accounting for known formula of differential geometry get the deformed length and curvature at each point s. Write the auxiliary expressions which are derived by differentiation of (9):

$$\dot{X}(s) = 1 - \dot{W}(s)\sin\theta(s) - W(x)\cos\theta(s)\dot{\theta}(s);$$

$$\dot{Y}(s) = \dot{W}(s)\cos\theta(s) - W(s)\sin\theta(s)\dot{\theta}(s).$$

They allow to find elongation, $\varepsilon(s)$, (relative change of length) of each point s:

$$\varepsilon(s) = \frac{\Delta s_d}{\Delta s} = \sqrt{(\dot{X})^2 + (\dot{Y})^2},$$

where Δs_d is the deformed length of initial element Δs. The curvature, $\kappa_d(s)$, of the curve (9) in each point is given by known expression:

$$\kappa_d(s) = \frac{\ddot{X}\dot{Y} - \ddot{Y}\dot{X}}{\left(\sqrt{(\dot{X})^2 + (\dot{Y})^2}\right)^3} = \frac{\ddot{X}\dot{Y} - \ddot{Y}\dot{X}}{(\varepsilon(s))^3} \qquad (10)$$

Expand the components of numerator (10) with accounting for known differential dependences (1):

$$X(s) = \ddot{M}(s)\sin\theta(s) + 2\dot{\theta}(s)\cos\theta(s)\dot{M}(s) -$$

$$- W(s)\sin\theta(s)(\dot{M}(s))^2 + W(s)\cos\theta \cdot \dot{Q}(s); \tag{11}$$

$$Y(s) = \ddot{M}(s)\cos\theta(s) - 2\dot{\theta}(s)\sin\theta(s)\dot{M}(s) -$$

$$- W(s)\cos\theta(s)(\dot{M}(s))^2 - W(s)\sin\theta \cdot \dot{Q}(s). \tag{12}$$

So, expressions (10) together with (11) and (12) allow to find the real curvature of curve (9).

Now introduce the notion of imaginary points. Theory of beams is based on assumption that calculated angles are small, i.e., $\theta \approx \sin\theta \approx \mathrm{tg}\,\theta$. If the number of points A_i is small, then misalignment angles are large (Fig. 1). Thus, calculated angles are also large which lead to some inaccuracy. To decrease these angles of misalignment it is suggested to introduce the imaginary support points. These supports have zero rigidities $C_i = 0$. Nevertheless, the number of segments becomes larger and angles of misalignments become smaller. In details, this crucial idea of the method will be illustrated on testing examples.

RECOVERY OF FIGURES FROM EXACTLY MEASURED POINTS

Example 1. Start with example when several points of the circle are given exactly. Let we have four points $B_1(x_1 = -2, y_1 = 1)$; $B_2(2,1)$; $B_3(2,-1)$; $B_4(-2,-1)$. Evidently, they are situated on the circle of radius $R = \sqrt{5} \approx 2.236$, thus the curvature κ is equal to $\kappa = 0.4472$.

When all points are given exactly (imaginary points are not exact) there is no necessity to perform the iteration procedure, because the result is obtained at once. The fourth Conjugation equation is used in form: $W_{i,1} = 0$.

The calculation results are shown on Fig. 3. Due to small number of input points the calculated figure is not continuous. This relates to the tangent C^1 and curvature (moment) C^2 continuity. The calculated values of moment (curvature) are constant and equal to $\kappa = 0.5235$, which is 17% higher than accurate value (Fig. 3, *b*). Note, that axis of abscise is related with the lengths of initial straight segments, formed by 4 input points and the whole length is equal to 4+2+4+2=12. The above values of $\kappa = 0.5235$ is the formal solution by the beam theory. The real curvatures are calculated by formulas (10). The graph of real curvatures is shown on Fig. 3, *c*, which extremal values notably differ from exact and beam ones.

To improve the results, employ the idea of imaginary points. Introduce one imaginary point at the middle of each calculated graph section between two real points (Fig. 3, *a*). Denote them as B_{1-2}, B_{2-3}, B_{3-4}, B_{4-1}. Determine their

coordinates. Connect consequently points B_1, B_{1-2}, $B_2 \ldots B_4$, B_{4-1}, B_1 and get the new graph for eight initial points (Fig. 4).
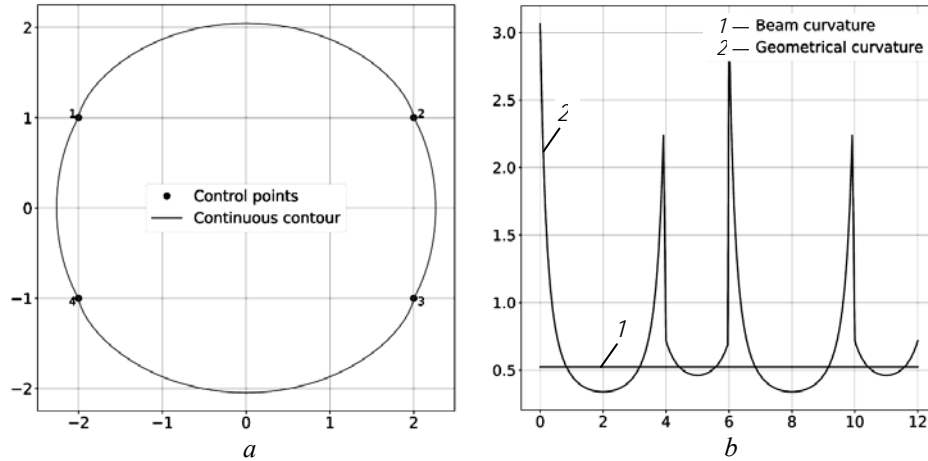

Fig. 3. Recovery of circle from 4 exactly measured points given as the vertices of the rectangle: *a* — calculated figure; *b* — beam and geometrical curvatures
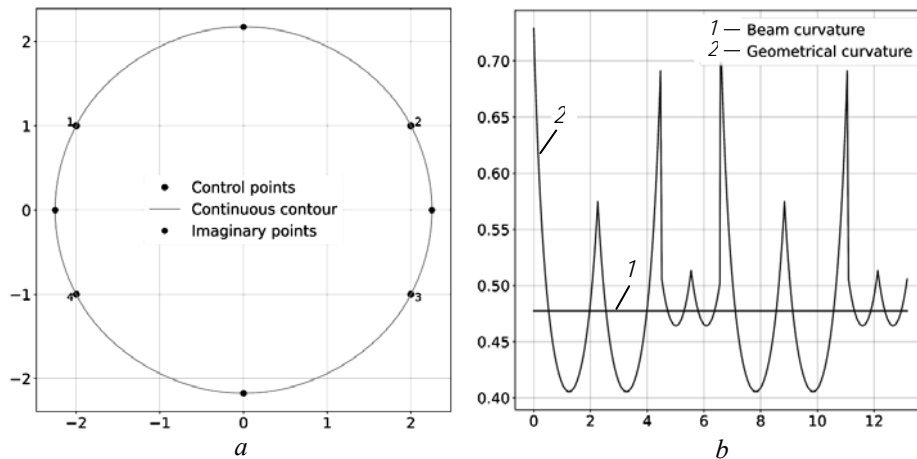

Fig. 4. Recovery of circle by four exact points and four imaginary ones: *a* – restored graph; *b* – recalculated curvatures by formula (10)

As we see the contour is more smooth, angular misalignments are almost invisible. The calculated beam curvatures are equal to 0.4773, which are 6.7% higher than exact ones. Yet the extremal geometrical curvatures given by formula (10) are still in 1.5 times higher than accurate value.

Therefore, insert additional 24 imaginary points – 3 points between the already used points – real and imaginary ones (Fig. 4). So, at the whole we get 4 real and 28 imaginary points. The results of calculation are shown on Fig. 5. The beam curvatures coincide with exact one (Fig. 5, *b*). The real curvatures after 3rd iteration are shown on Fig. 5, *a*. In this case they better correspond to the exact ones and the difference does not exceed 2%.

One may get the false impression that the accuracy of reproduction of calculated contour is related to the accuracy of preliminary placement of imaginary points. To show that crucial is only the fact of their insertion rather than place of placement, make the following test. Consider the contour obtained from

32 points (4+28), Fig. 5, *a*. For convenience consequently renumerate them starting from real point B_1. Artificially shift points N4, N14, and N26 outwardly, as shown on Fig. 6, *a*. From these points, we will form an initial polygon, which is the initial input geometry.
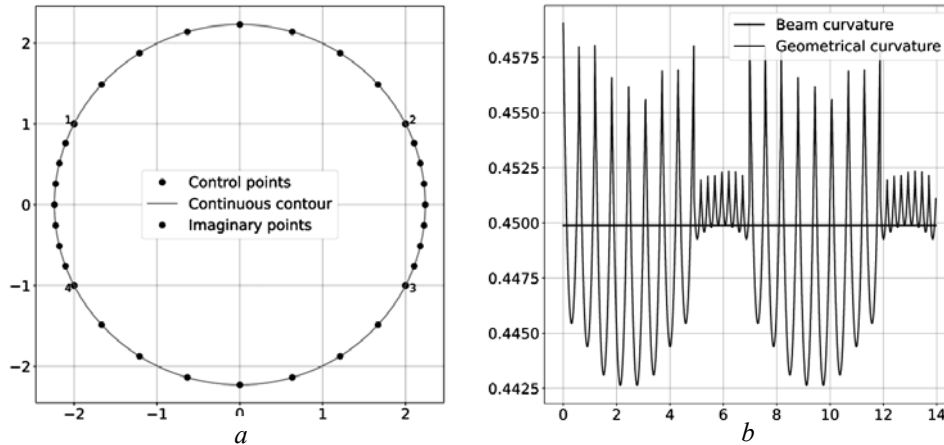

Fig. 5. Recovery of circle by 4 real and 28 imaginary points: *a* — calculated graph; *b* — recalculated curvatures by formula (10)

The calculated contours for some iterations are shown on Fig. 6. In particular, after first iteration the contour contains local loops, Fig. 6, *b*. After second iteration the contour resemble a slightly oval contour, Fig. 6, *c*. The contour become better with each subsequent iteration and after 6th iteration it is almost indiscernible from the ideal circle. After 9th iteration the correctly calculated curvatures are very close to the exact ones and differ with them only by 1–2%. Thus, availability of 32 points (real or imaginary) is almost enough to get the ideal circle. This means, that in overage $360/32 \approx 12°$ (and lesser) angular misalignment can be effectively smoothed by our modified beam approach.

Example 2. Consider the circle formed by unevenly placed points. In practice the measurements are often performed with some restrictions, when the available to measurements is only some segment of the circle. Set three points (Fig. 7), namely $B_1(x_1 = -\sqrt{3}/2, y_1 = 1/2)$; $B_2(0,1)$; $B_3(\sqrt{3}/2,1/2)$. Evidently these points belong to the circle of radius 1, and curvature is also 1. Note, that these points embrace only the 1/3 of the full circumference. Due to unevenness of their placement, the angular misalignments between the straight segments are: between the first and second ones – angle is $60°$, between second and third -120°, and third and first ones – $120°$. When the angle is larger than $90°$, the sense of beam theory is lost – angle does not only essentially differ from its tangent, but they have the different sighs. Therefore, from the start insert only one imaginary point, for example, $B_{3-1}(0,-5)$. The results are shown on Fig. 7. Evidently, the contour contains the loop and do not resemble the circle at all.

Consider the calculated contour Fig. 7, *b* as initial one, and insert between the real points B_1 and B_2 and point B_2 and point B_3 15 additional imaginary points, also insert 26 points between the points B_3 and point B_{3-1}, the same is between B_{3-1} and B_1. The calculation is performed at several iterations, until the

stabilization of the geometry (Fig. 8). The derived geometry, which contains 3 real and 83 imaginary points, is very close to the ideal circle, Fig. 8, *a*. As to beam curvatures they differ only by 0.1% from exact ones, while the geometrical curvatures are slightly worse – the difference reach up to 0.3%.
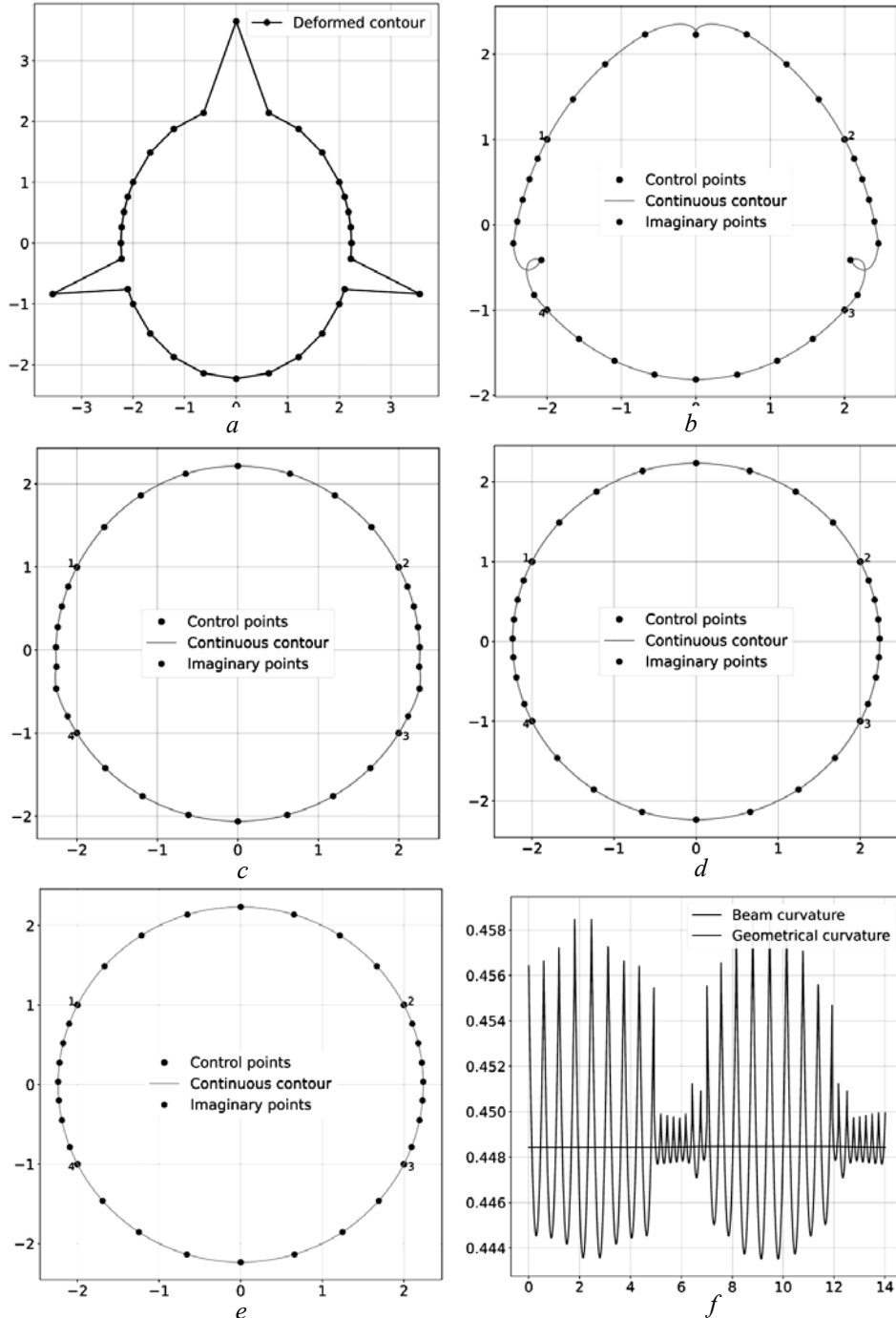

Fig. 6. Recovery of circle from 4 real and 28 imaginary points, three of which were essentially shifted: *a* — initial placement of points; *b* — contour after 1st iteration; *c* — after 2nd iteration; *d* — after 6th iteration; *e* — after 9th iteration; *f* — calculated by (10) curvatures after 9th iteration
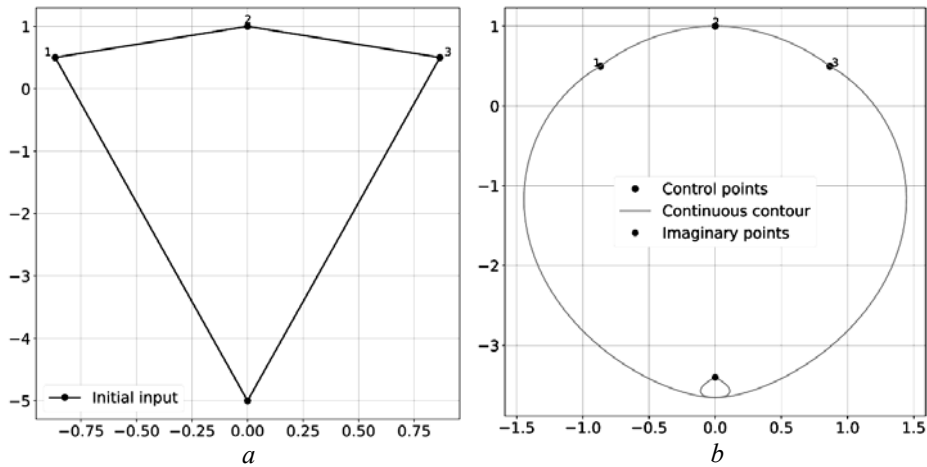
Fig. 7. Recovery of the circle from 3 real points placed at the upper part of circle and one imaginary point: *a* — input point; *b* — calculated contour with loop
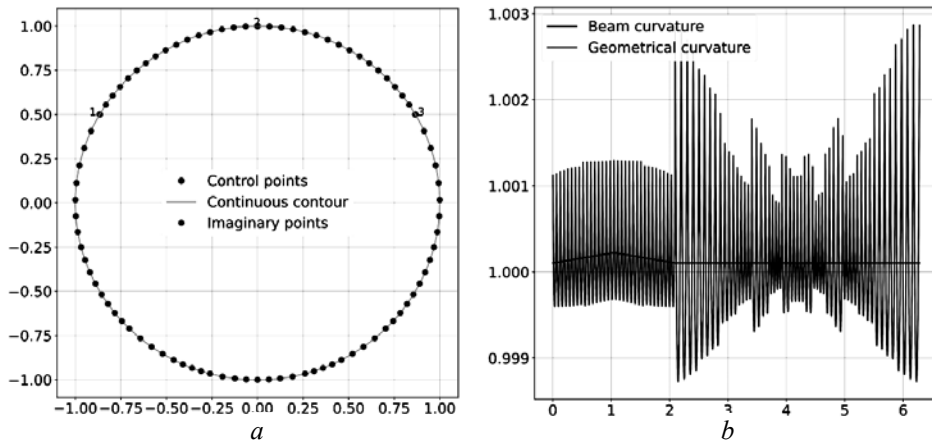

Fig. 8. Recovery of circle from 3 real points and 83 imaginary ones: *a* — calculated contour; *b* — beam and geometrical (10) curvatures

Example 3. Here we consider a more complicated figure – ellipse. In contrast to the circle, its curvature is not a constant. So, it is interesting to explore the ability of the method to restore the figures with variable curvature. Use the equation of ellipse with respect to parameter φ, where the coordinates of any point are given by equations: $x = 2 * \cos(\varphi)$ and $y = 1 * \sin(\varphi)$. The curvature of ellipse is given by the following expression:

$$\kappa(\varphi) = \frac{a * b}{\sqrt{a^2 - (a^2 - b^2)(\cos(\varphi))^2}^3} \, . \tag{13}$$

Note, that in point $\varphi = 0$ $\kappa(0) = \dfrac{a}{b^2} = 2$, and value of $\kappa(\pi/2) = \dfrac{b}{a^2} = \dfrac{1}{4}$. So, the curvature changes in 8 times within the range of 90 degrees.

Generate 40 points (10 points for each quadrant), between which the curvature changes proportionally, i.e., in $k = \sqrt[10]{8}$ times. These points (their parametric values of φ_i) are easily generated from equation (13). Fig. 9 shows the positions

of 40 generated ellipse points and corresponding calculated contour and its beam and geometrical curvatures. In general, we see a very good correspondence, with the exception of points which lays on axis x, where the real curvature is the largest. Here the deviation of geometrical curvature from the exact one attains 10%. Of course, these results can be improved by taking more input points in the vicinity of point $\varphi = 0$. Yet, in general, the results are very optimistic, even for figure with quickly changing curvature.
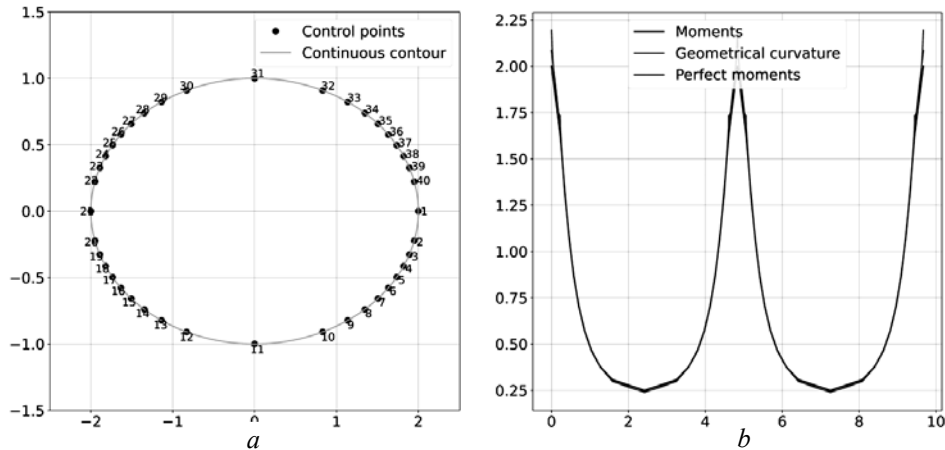

Fig. 9. Recovery of ellipse from exactly placed discrete points: *a* — input points and calculated contour; *b* — graph of exact curvature of ellipse and its calculated beam and geometrical curvatures

RECOVERY OF THE CIRCLE FROM NOISY POINTS

Example 4. Consider again the ideal circle of radius 1. Take 40 evenly distributed points on it. Then add the noise to each coordinate of point (X and Y) according to uniform continuous distribution with random parameters ranged from lower boundary $a = -0.3$ to upper boundary $b = 0.3$. The noise is characterized by theoretical statistical deviance:

$$\sigma_{theor} = \frac{(b-a)}{2\sqrt{3}}.$$

So, in our case $\sigma_{theor} = 0.173$.

The input random points are given in Table .Their sequence does not resemble the ordered one, where each next enumerated point is placed in clockwise direction from the previous one. So, their placement sometimes looks as chaotic one, which complicates the calculations. The results of calculations are shown on Fig. 10. A large number of closed loops are formed at first iteration. Then, with decreasing of the spring rigidity their number decreases, and the reason is the overlapping of the points which form the loops. The loops are completely unraveled at 15th iteration when $\overline{C} = 0.473$. With subsequent iterations the contour more and more resembles a perfect circle. The calculations are ceased at 40th iteration when $\overline{C} = 3.3310^{-5}$.

Introduce the notion of conditional empirical calculation deviance, σ_{emp}, i.e., root mean square deviation of input points B_i from the calculated contour, which we approximately define by formula
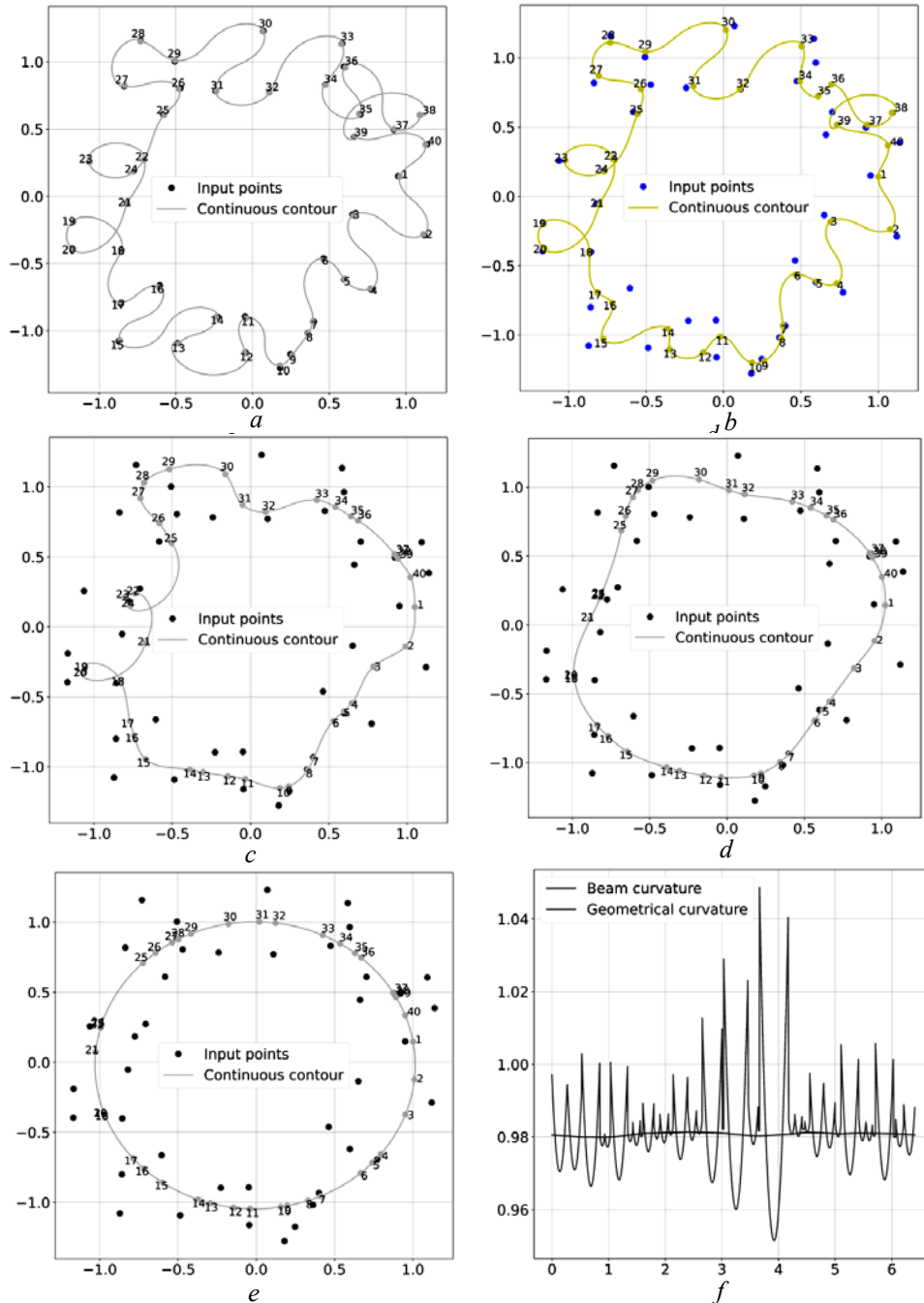

Рис. 10. Recovery of circle from 40 noised points generated by uniform distribution law with an extremal deviation equal to ± 0.30: a — input points and contour at 1st iteration; b — contour after 5th iteration, $\overline{C} = 21.66$; c — after 12th iteration, $\overline{C} = 1.49$; d — after 15th iteration, $\overline{C} = 0.47$; e — after 40th iteration $\overline{C} = 3.33 \cdot 10^{-5}$; f — the beam and geometrical (10) curvatures after 40th iteration

Generated 40 random points with respect initial 40 evenly chosen points on the circle

N	X	Y	N	X	Y	N	X	Y	N	X	Y
1	0.9616	0.0000	11	0.0727	-1.2507	21	-0.9969	0.0611	31	-0.0193	0.8941
2	0.7032	0.0773	12	-0.1389	-1.0679	22	-1.2485	0.3154	32	-0.0225	0.8435
3	0.9809	-0.4040	13	-0.5283	-0.7405	23	-0.9942	0.1106	33	0.3933	0.8832
4	0.8522	-0.4137	14	-0.4458	-0.9472	24	-1.1331	0.3298	34	0.4438	1.0902
5	0.7612	-0.6313	15	-0.7771	-1.0927	25	-1.0327	0.6022	35	0.5909	0.9511
6	0.6053	-0.7451	16	-0.5359	-0.8588	26	-0.6491	0.6211	36	0.6392	0.6346
7	0.4106	-0.6431	17	-0.5966	-0.8475	27	-0.7522	0.5364	37	0.9852	0.2956
8	0.5256	-0.8696	18	-0.8945	-0.1577	28	-0.6898	1.1809	38	0.9390	0.6324
9	0.1888	-0.6788	19	-0.7431	-0.0267	29	-0.4768	0.9159	39	0.7484	0.1707
10	0.0165	-0.9612	20	-1.2399	0.0237	30	-0.2465	0.9901	40	1.1081	0.2060

$$\sigma_{emp} = \sqrt{\frac{\sum_1^N \Pi_i^2}{N}} \ . \qquad (14)$$

Calculate this value by formula (14) at the last (40th) iteration. Empirical deviation is equal to $\sigma_{emp} = 0.151$, which is very close to the theoretical deviance. Such good correspondence is due to the big number of input points, and that conditional distance Π_i reflects the essence of the distance to the contour. Underline, that above example illustrates that attained empirical deviance at the given iteration σ_{emp} can be used as a condition of termination of smoothing process, provided that theoretical deviance is known.

EXTRACTION OF SILHOUETTES FROM NOISY POINTS [4]

Example 5. The problem of recovery of silhouettes from noisy dense points was considered in work [4]. Among other, this work is remarkable that it gives a lot of sets of artificially generated random points from continuous silhouettes, yet the original silhouettes were not provided. Unknown is also the principle of the random points generation. In the title of respected files, which were supplemented to work [4], there are some numerical values of errors which can be treated as deviance of input points. Other problem with these data is the numeration of points. Our method works with numerated points and does not change their numeration. But as is shown in Example 4 when points are very dense noisy, the renumeration is desirable. Yet, in this work we will not apply the renumeration procedure, to show that our method is very effective even without it.

Consider first figure from work [4] — butterfly. Input noisy data are given in the file (butterfly_2percent_noise.txt"), where 164 points are presented. The mentioned in the file name noise is given in percent. Due to that all pictures are given in absolute coordinates which range approximately from -0.5 to $+0.5$ as for x as for y, thus we assume that deviance was calculated relatively to the value of 0.5. Thus, we take that theoretical deviance is equal to $\sigma_{theor} = 0.02 \, 0.5 = 0.01$.

The results of calculation are given on Fig. 11. Initial input points are presented on Fig. 11, *a*. The results of calculation after 1ˢᵗ iteration are shown on Fig. 11, *b*, where three local loops are presented, and the empirical deviance is
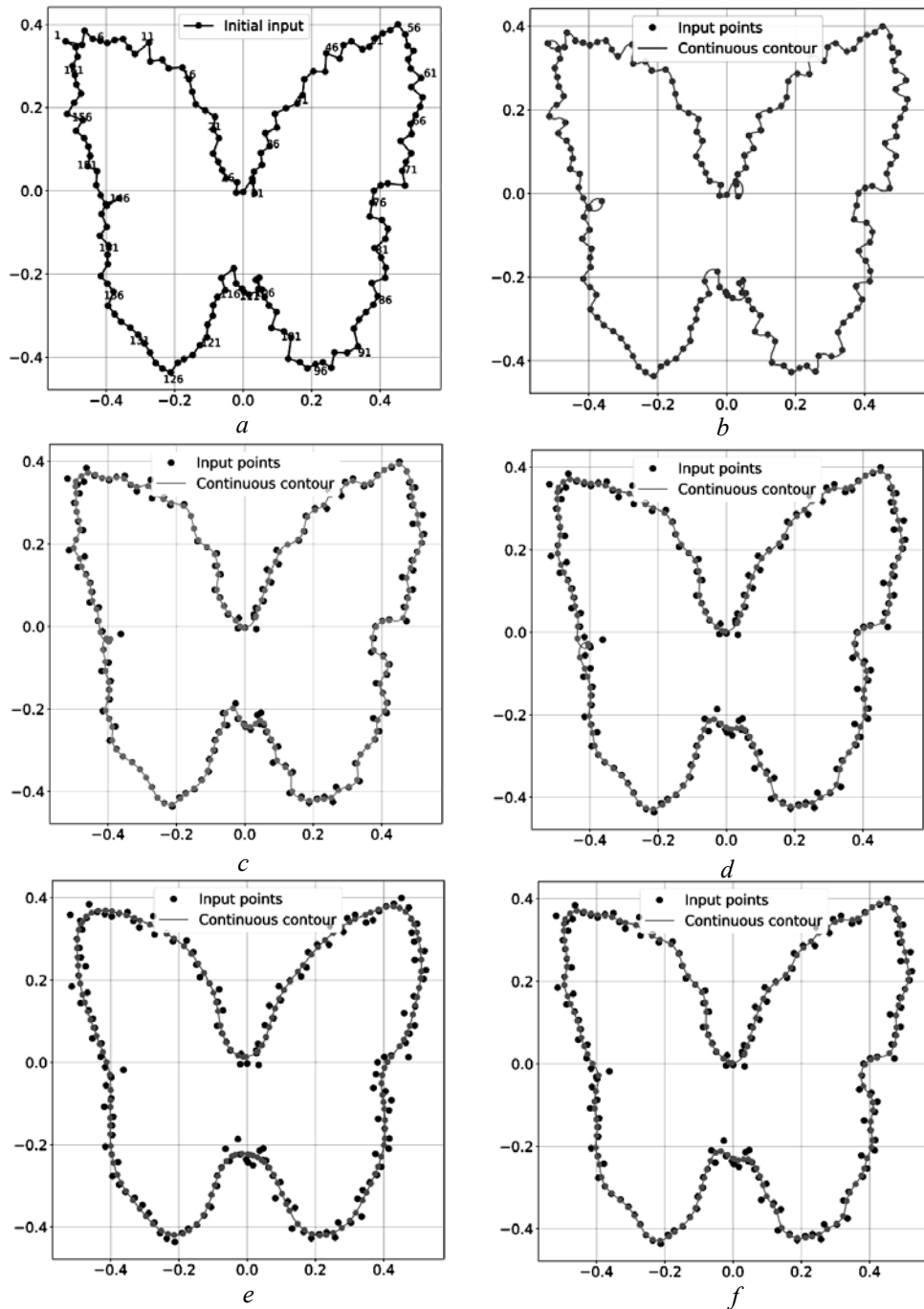

Fig. 11. Recovery of contour of butterfly based on input points given in [4]: *a* — initial points; *b* — contour after 1ˢᵗ iteration; *c* — after 15ᵗʰ iteration, $\overline{C} \approx 1.64$; *d* — after 20ᵗʰ iteration, $\sigma_{emp} \approx 0.010$, $\overline{C} \approx 0.377$; *e* — after 30ᵗʰ iteration, *f* — returning to the same rigidity as at 20ᵗʰ iteration, $\sigma_{emp} \approx 0.010$

very small and equal to $\sigma_{emp} = 0.00029$. After 15th iteration the contour still has one small loop (at the left side of picture) and calculated deviance becomes $\sigma_{emp} = 0.00672$, which is less than assumed theoretical value. Interesting to notice, that the contour doesn't look smooth enough. At 20th iteration ($\overline{C} = 0.377$), the calculated value $\sigma_{emp} = 0.01060$, which is very close to the criterial value. Yet the contour still contains one local loop; to unravel it perform the several additional calculations. At 30th iteration $\sigma_{emp} = 0.01378$, which is larger than theoretical one, which testifies about the oversmoothing of the contour, what is subjectively visually confirmed. It is interesting to note, that we can return from 30th iteration's rigidity to the 20th iteration's rigidity (which is equal to $\overline{C} = 0.377$). In this last case the calculated value of $\sigma_{emp} = 0.01059$, yet the local loop has disappeared.

Consider the data for crab [4], ("crab_2percent_noise.txt"), Fig. 12, where 284 points are given. The theoretical deviance is taken to be $\sigma_{theor} = 0.01$. The larger number of points might lead to the increase of the number of local loops at first iterations. The results at first iterations are presented on Fig. 12, *b*, where input points and calculated contour points almost coincide. The value of calculated deviance $\sigma_{emp} = 0.00032$ is very small due to large rigidity of supports, yet contour has four local loops. At 15th iteration the contour still has some visual misalignments, and the calculated deviance is equal to $\sigma_{emp} = 0.01051$, which is close to the theoretical one. Besides, contour still has one loop. At 18th iteration the calculated and theoretical deviances are almost the same, but contour still contain the loop. At 30th iteration the calculated $\sigma_{emp} = 0.01716$, which is larger than the theoretical one, and visually the contour looks like the oversmoothed one. Therefore, we start to change the supports rigidity in inverse order. Fig. 12, *f* shows the calculated contour when the rigidity $\overline{C} \approx 1.22$, which is the same as in direct order 16th iteration. Here the value of $\sigma_{emp} = 0.01049$, which is very close to the theoretical one. So, contour of Fig. 12, *f* can be considered as the good result of smoothing.

Consider the figure of dolphin [4] ("dolphin_2percent_noise.txt"), Fig. 13, 179 points, $\sigma_{theor} = 0.01$. There are 3 local loops at 1st iteration, Fig. 13, *b*. Calculated deviance after 15th iteration at $\overline{C} = 1.64$ is equal to $\sigma_{emp} = 0.0086$, which is slightly less than the theoretical one. At 18th iteration $\sigma_{emp} = 0.0102$ and is close to theoretical one. At 30th iteration the deviance $\sigma_{emp} = 0.0165$, which testifies that contour is oversmoothed, and this is visually confirmed. Increasing the iteration number (decreasing the rigidity) lead to additional oversmoothing. As example, consider the contour obtained after 60th iteration at $\overline{C} = 2 10^{-5}$, where $\sigma_{emp} = 0.08902$, which is one order higher than the theoretical one. Evidently, the

peculiarity of the method is that at very small number of rigidity it eventually gives the perfect circle. So, the criteria of termination should be specified.
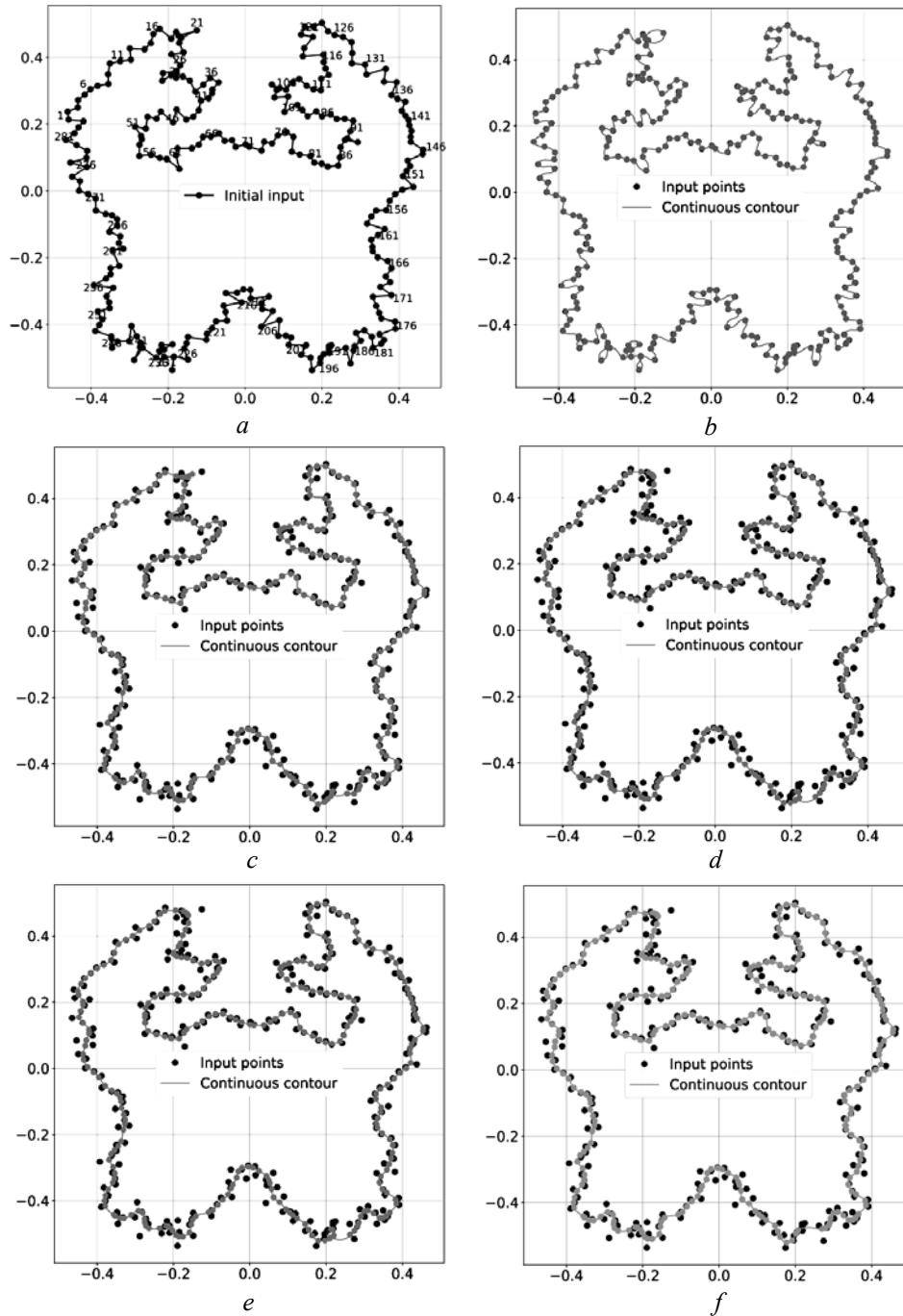

Fig. 12. Recovery of the contour of crab based on data of [4]: *a* — nitial points; *b* — contour after 1st iteration; *c* — after 15th iteration; *d* — after 18th iteration, $\sigma_{emp} \approx 0.010$; *e* — after 30th iteration; *f* — reverse increasing of rigidity till the value as in direct smoothing after 16th iteration, $\sigma_{emp} \approx 0.010$
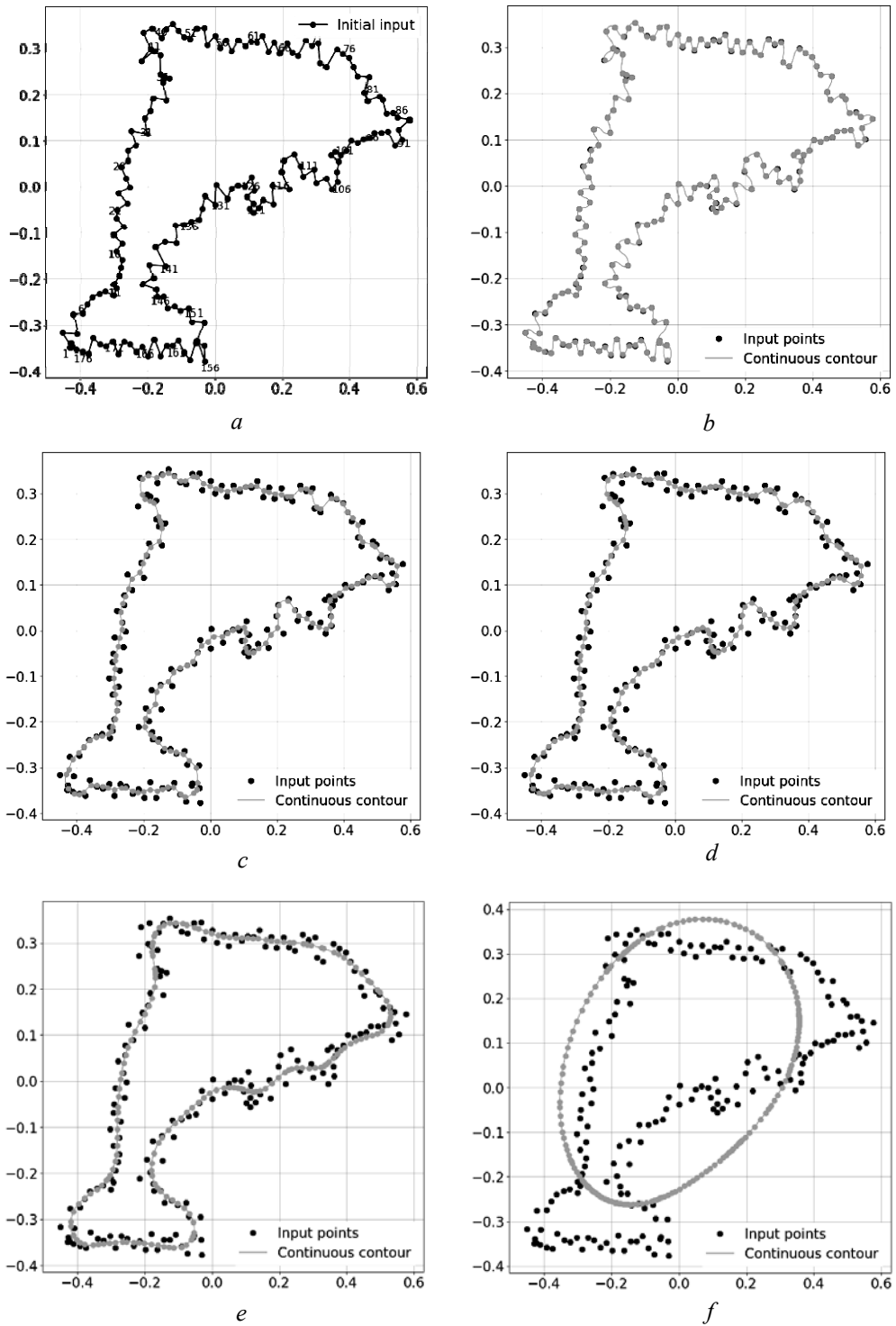
Fig. 13. Recovery of dolphin contour based on data of work [4]: *a* — input data; *b* — contour after first iteration; *c* — 15th iteration, $\sigma_{emp} = 0.0086$; *d* — 18th iteration, $\sigma_{emp} = 0.0102$; *e* — 30th iteration $\sigma_{emp} = 0.0165$; *f* — 60th iteration, $\sigma_{emp} = 0.08902$

CONCLUSIONS

Based on the authors' experience in the field of structural mechanics the principally new methods of smoothing the noisy data to get the continuous closed contours is proposed. The following results are obtained:

Based on the theory of straight beams, which lays on discrete elastic supports with finite rigidity, the general governing equations are formulated. They include 4 Connection equations for each straight beam segment and 4 Conjugation equations, which should "match" the end of previous segment with the beginning of subsequent one. The last one among other serves to smooth the angle of misalignment between two neighboring segments, which is attained by corresponding requirements to the angular deformations of segments at their border.

The notion of imaginary points is suggested, which broke the segment on two smaller one but do not envisage the insertion of the additional support between them. They are introduced when the angular misalignment between two adjacent segments is large. Their availability is very instrumental in providing the C^2 continuity of the smoothed contour.

The algorithm of refinement of calculated positions of the points of segment is proposed. It accounts for by rotating the initial normal vector to the segment on the calculated deformation angle in each point. This serves to provide the continuity of the contour points. The iteration process of refinement of the contour which consists in consequent process of the decreasing the support rigidities is proposed. Its efficiency is confirmed to analysis of very dense and noisy input points, where the local loops may occur at initial stages of algorithm.

The notion of experimental (calculated) statistical deviance from the initial input points is suggested. It is shown that for attainment the visually best smoothing this value should be close with the theoretical (generated) deviance of input points. So, this value can be used for formulation of the criteria of formal termination of smoothing procedure.

REFERENCES

1. D.F. Rogers, *An Introduction to NURBS With Historical Perspective*. San Diego, CA: Academic Press, 2001.
2. Mark S. Nixon and Alberto S. Aguado, *Feature Extraction & Image Processing for Computer Vision*. Academic Press, 2013, 609 p. doi. 10.1016/C2011-0-06935-1.
3. T. Strutz, *Data Fitting and Uncertainty: A Practical Introduction to Weighted Least Squares and Beyond*. Wiesbaden, Germany: Vieweg, 2010.
4. Stefan Ohrhallinger and Michael Wimmer, "StretchDenoise: Parametric Curve Reconstruction with Guarantees by Separating Connectivity from Residual Uncertainty of Samples," *PG '18: Proceedings of the 26th Pacific Conference on Computer Graphics and Applications: Short Papers, October 2018*, pp. 1–4. Available: https://doi.org/10.2312/pg.20181266
5. Ahlberg J. Harold, Edwin Norman Nilson, and Joseph Leonard Walsh, "The theory of splines and their applications," *Mathematics in Science and Engineering*, 1967.
6. Stephen P. Timoshenko, Strength of materials. Part 1: Elementary theory and problems, 1955.
7. D.G. Schweikert, "An interpolating curve using a spline in tension," *J. Math. Physics*, 45, pp. 312–317, 1966.

8. P.H. Wagner, X. Luo, and K.A. Stelson, "Smoothing curvature and torsion with spring splines," *Computer-Aided Design*, vol.27, no. 8, pp. 615–626, 1995. doi: 10.1016/0010-4485(95)99798-D.

9. I. Orynyak, I. Lokhman, and A. Bohdan, "The Spring Splines Procedure with Prescribed Accuracy for Determination of the Global (Pipe Centerline) as well as the Local (Dent) Curvatures," *Proceedings of IPC 2012 9th International Pipeline Conference, September 24–28, Calgary, Alberta, Canada, IPC2012-90127*. doi: 10.1115/IPC2012-90127.

10. I.V. Orynyak, I.V. Lokhman, and A.V. Bogdan, "Determination of curve characteristics by its discrete points measured with an error and its application to stress analysis for buried pipeline," *Strength of Materials*, 44(3), pp. 268–284, 2012. doi: 10.1007/s11223-012-9380-7.

11. M.A. Crisfield, "A consistent co-rotational formulation for non-linear, three-dimensional, beam-elements," *Computer Methods in Applied Mechanics and Engineering*, vol. 81, issue 2, pp. 131–150, 1990. doi: 10.1016/0045-7825(90)90106-V.

12. I. Orynyak, R. Mazuryk, and A. Orynyak, "Basic (discontinuous) and smoothing up (conjugated) solutions in transfer matrix method for static geometrically nonlinear beam and cable in plane," *Journal of Engineering Mechanics*, 146(5), 2020. doi: 10.1061/(ASCE)EM.1943-7889.0001753.

INFORMATIONON THE ARTICLE

Igor V. Orynyak, ORCID: 0000-0003-4529-0235, National Technical University of Ukraine "Igor Sikorsky Kyiv Polytechnic Institute", Ukraine, e-mail: igor_orinyak@yahoo.com

Dmytro R. Koltsov, ORCID: 0000-0002-0396-7255, National Technical University of Ukraine "Igor Sikorsky Kyiv Polytechnic Institute", Ukraine, e-mail: koltsovdd@gmail.com

Oleg R. Chertov, ORCID: 0000-0003-0087-1028, National Technical University of Ukraine "Igor Sikorsky Kyiv Polytechnic Institute", Ukraine, e-mail: chertov@i.ua

Roman V. Mazuryk, ORCID: 0000-0003-4309-824X, National Technical University of Ukraine "Igor Sikorsky Kyiv Polytechnic Institute", Ukraine, e-mail: r.mazuryk.ua@gmail.com

ЗАСТОСУВАННЯ ТЕОРІЇ БАЛОК ДЛЯ ПОБУДОВИ ПЛОСКИХ ДВІЧІ ДИФЕРЕНЦІЙОВАНИХ ЗАМКНУТИХ КРИВИХ ЗА НЕТОЧНИМИ ДИСКРЕТНИМИ ДАНИМИ / І.В. Ориняк, Д.Р. Кольцов, О.Р. Чертов, Р.В. Мазурик

Анотація. Згладжування дискретних точок, заміряних з певною похибкою, має велике значення в різних технічних застосуваннях та комп'ютерній графіці. Ідея роботи полягає в застосуванні методів теорії балок на пружних опорах. Установлюються локальні системи координат для прямолінійних відрізків балок, де кути неспіввісності згладжуються відповідними умовами в рівняннях спряження. Для наближення довжини отриманого контуру до довжини прямолінійних балок уводиться поняття умовних точок, що розміщуються між точками замірів. Наводиться ряд прикладів реконструкції реальних контурів по заміряних дискретних точках із заданою і невідомою похибками.

Ключові слова: сплайн, пружна балка, опора, замкнутий контур, уявна точка, неточні дані.